Jordan Journal of Civil Engineering, Volume **3**, No. **4**, **2009**

Effect of Welding on Lateral-Torsional Buckling Resistance of I-Shaped Built-up Steel

Raja M. Younes [1)]***, Ghazi Abu-Farsakh*** [2)] ***and Yasser M. Hunaiti*** [3)]

[1)] Department of Civil Engineering, Tafila Technical University, Jordan
[2)] Department of Civil Engineering, Jordan University of Science and Technology, Jordan
[3)] Department of Civil Engineering, University of Jordan, Jordan

ABSTRACT

An experimental investigation was made of the inelastic lateral-torsional buckling of built-up steel I-beams. All beams were carefully fabricated with controlled levels of initial crookedness. Nineteen beams were tested in five groups under same loading conditions with two points load applied at the top flange. The results confirmed that built-up beams of intermediate slenderness with fillet welds on one side of the web are sometimes stronger than their counterpart beams with fillet welds on both sides of the web. It was found that design loads predicted by the Australian Standard provided good lower bounds estimates to failure loads of the tested beams.

KEYWORDS: Welding, Lateral-torsional buckling, I-beams.

INTRODUCTION

One of the key feathers of metal building systems is their primary frames being made up of built-up plate rigid frames. Steel plates are cut into tapered shapes for webs and prismatic shapes for flanges. Then these shapes are placed into a ConRac submerged arc welder that welds both flanges to the web at one time. Since the primary cornerstone of metal building construction is to minimize the building cost, the goal is usually achieved through optimization of steel weight and the fabrication process by adopting the built-up I-shaped web-tapered primary framing members with bolted end-plate connections and using fillet welds on one side of the web. This method of fabrication (connecting the flange and the web by using fillet welds on one side of the web instead of two sides) and its effect on stability of the members are not explicitly explained in the related specifications. Moreover, limited information about this subject causes ambiguity among practicing engineers. In view of the limited information available on the behavior of built-up steel beams with one fillet welds on one side of the web, nineteen buckling tests were carried out on five groups of built-up I-beams with two symmetrical concentrated loads applied vertically at the third point of the compression flange.

Over the past several years, the lateral–torsional buckling of beams of rigid cross section has been thoroughly investigated and summarized in many text books (Timoshenko and Gere ,1961; Galambos, 1988; Trahair, 1993), while methods of design are presented in modern standards (Load Resistance Factor Design specification LRFD (2003); European Standard Eurocode 3 (2005), Part 1.1; Canadian Standard CSA-S16-01 (2001); Australian Standard AS4100 (1998)).

Tests on lateral torsional buckling of I-beams were

Accepted for Publication on 1/10/2009.

focused on hot-rolled sections or welded sections with fillet welds on both sides of the web (Fukumoto and Kubo, 1977; Fukumoto *et al*., 1980,1982; Fukumoto and Itoh, 1981; Fukumoto and Kubo *et al*., 1988).

There does not appear to be any published data in the international literature on lateral buckling of doubly-symmetric I-beams with fillet welds only on one side of the web.

MATERIAL PROPERTIES AND RESIDUAL STRESSES

Material Properties

Thirteen tension tests were carried out on specimens prepared from the original plates to determine their material properties. The coupons were prepared and tested in accordance with ASTM E8 Standard Test Methods and Definitions for Mechanical Testing of Steel Products (ASTM, 2003). All the tensile coupons were tested in a 2000 kN capacity Universal Testing Machine. The main yield stress was 378 MPa, the mean value of Young's modulus was 204000 MPa and the Poisson's ratio was 0.29.

Residual Stresses

The residual stresses were measured at three points (1, 2 and 3) as shown in Fig. (1). The measurements were based on the drill hole method. Strain gages EA-06-062RE-120 were used. The drill hole rosette requires a small drill hole of about 2 mm in diameter. This can be regarded as a non-destructive technique (ASTM Standard E837, 2001). The average measured values were used to represent the residual state of the tested beams and are listed in Table (1).

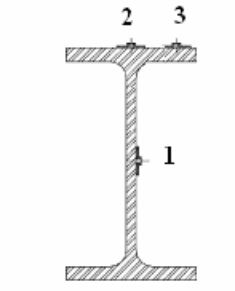

Figure (1): Points of Measurement of the Residual Stresses.

Table (1): Experimental Results of Residual Stresses.

Specimens	Point 1 MPa	Point 2 MPa	Point 3 MPa
A30	-11	135	-92
AA30	-40	195	-192
B40	-14	216	-113
BB40	-153	292	-116

LATERAL BUCKLING TESTS

Test Beams

To study the lateral buckling behavior of simply supported built-up beams with fillet weld: 1) on one side of the web; 2) on both sides of the web as shown in Fig. (2), nineteen buckling tests were carried out on five groups of built-up I-beams with two symmetrical concentrated loads applied vertically at the third point of the compression flange.

All specimens in this research were carefully fabricated with controlled levels of initial crookedness to reduce its effect on load capacity of the beam in order to clarify the effect of residual stresses. Straight specimens were fabricated such that the maximum offset of each flange was less than L/1000, in which L is the distance between points of lateral support, corresponding to the fabricated tolerance limits specified in (AS4100, 1998).

A pair of transverse stiffeners was attached to the web at the loading points. Fillet weld of size 5 mm leg length was used for all specimens. All welding was performed in accordance with AWS structural welding Code D1.1-2000 (AWS, 2000). The ratio of thicknesses of the flange and the web (t_f / t_w) was varied from 1.2-1.33, while the ratio (b_f / h) was varied from 0.39-0.52. The values of width-thickness ratio of the flanges ($b_f / 2t_f$) were approximately 9, 12 and 14, and those of the webs (h / t_w) were approximately 60, 75 and 77. The span lengths L of the beams were such that the lateral torsional-buckling failure occurred in the inelastic region, and the slenderness ratios, L / r_y (r_y = the radius of

gyration about the minor axis), were approximately 60, 67, 90 and 100. The measured dimensions of all the tested beams are listed in Table (2). Specimen with the letter A at the end of its name means fillet welds on both sides of the web.

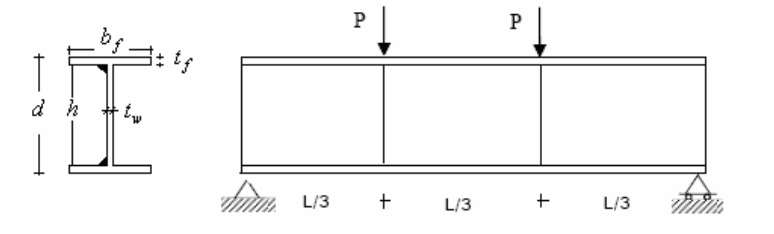

Figure (2): Beam Specimens with Fillet Weld on One Side of the Web.

Table (2): Dimensions of Beam Specimens.

Group	Specimens	d mm	b_f mm	t_f mm	t_w mm	$b_f / 2t_f$	h / t_w	L m	L / r_y
1	AB1	300.10	150.80	4.10	5.30	14.23	70.61	2	60.9
	AB2	300.12	150.94	4.20	5.27	14.32	68.95	2	61.2
	AB1A	300.14	150.44	4.30	5.22	14.41	67.37	2	62.2
	AB2A	300.17	150.58	4.25	5.35	14.07	68.11	2	61.6
2	BB1	400.11	150.13	5.11	6.04	12.43	75.94	2	66.9
	BB2	400.20	150.00	5.14	6.12	12.25	75.48	2	66.9
	BB1A	400.13	150.11	5.03	6.12	12.26	77.12	2	66.7
	BB2A	400.15	149.99	5.11	6.14	12.21	75.90	2	66.9
3	AB3	300.10	150.14	4.20	5.15	14.58	69.00	3	92.9
	AB3A	300.20	150.10	4.13	5.10	14.72	70.22	3	93.2
	AB4A	300.00	150.20	4.00	5.20	14.44	72.40	3	92.1
4	BB3	400.23	150.20	5.15	6.20	12.11	75.31	3	99.9
	BB4	400.15	150.13	5.18	6.10	12.31	74.89	3	100.5
	BB3A	400.10	150.02	5.17	6.14	12.21	75.01	3	100.7
	BB4A	400.10	150.03	5.22	6.10	12.29	74.31	3	101.1
5	CB3	400.17	150.12	6.18	8.11	9.26	62.16	3	97.5
	CB4	400.1	150	6.14	8.08	9.28	62.56	3	97.5
	CB3A	400.21	150.14	6.11	8.13	9.23	62.9	3	97.4
	CB4A	400.01	150.2	6.2	8.1	9.27	61.94	3	97.7

Supported System

Specially designed supports as shown in Fig. (3) with a horizontal axis and a vertical axis have been fabricated to approach the simply supported conditions in-plane and out-of-plane. It can be seen from Fig. (3) that the test beams were simply supported both in-plane and out-of-plane. The in-plane vertical deflections were prevented by the supporting sides with bolted end-plate connections. The in-plane rotations were not restrained because the beam could rotate freely about the horizontal axis ($x_1 - x_1$) through two roller bearing. The out-of-plane deflection and twist rotation were prevented. The minor axis rotations were not restrained because the beam could rotate freely about the vertical axis ($y_1 - y_1$) through a thrust ball bearing which transmits the end reaction. The two support ends were the same except that the beam at one end was prevented from running by horizontal stops while the beam at other end was allowed to run.

Figure (3): Support System.

Test Set-Up

Experimental tests were carried out in a rig (designed and fabricated in DARTIC, limited). This rig consists of two portal frames, supports, a strong floor with matrix of fixing holes in both directions @ 500 mm and two loading hydraulic actuators, where each of these actuators had a load capacity of 417 kN in compression and a built-in load cell. Figs. (4) and (5) show elevation, instrumentation, supports and details of the set up.

Instrumentation

The test specimens were instrumented with a variety of sensors. The targeted measurements include load measurements, displacement measurements and strain measurements. The nineteen built-up beams were instrumented at different selected positions to obtain the data necessary to describe their strength and behavior. All electronic measuring devices such as load cells, Linear Variable Displacement Transducer LVDTs, and cable transducers were calibrated before use.

Load Measurements

The two hydraulics actuators were provided with load cells which furnished direct measurements of the applied vertical forces. The loading cells are connected to the data acquisition system.

Displacement Measuring Instruments

Measurements of the horizontal and vertical deflections of the central section of the selected beams in each group were obtained by using Linear Variable Displacement Transducer LVDTs. An LVDT is composed of a metal barrel out of which a metal piston protrudes. When this piston moves, it causes a change in potential which in turn is a measure of displacement. Four LVDTs were used to measure displacement at different positions for each specimen. Three vertical LVDTs were used to measure vertical displacements at supports and mid span, respectively. In addition, one horizontal LVDT was attached to the top fiber of the compression flange at mid span to measure lateral deflection. The general arrangement of LVDTs as installed on the specimens is shown in Fig. (4).

Strain Measurement

Electric resistance strain gages of type AP-11-S300N-

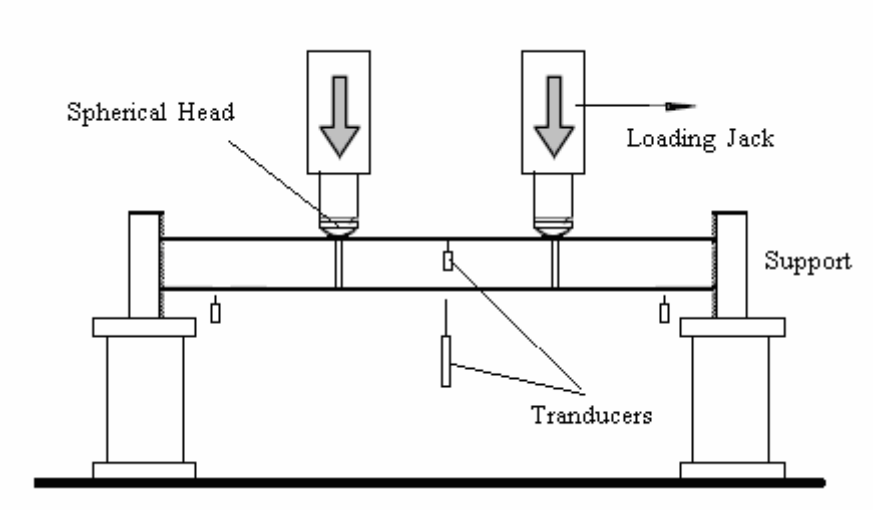

Figure (4): Schematic Diagram of Test Set-Up.

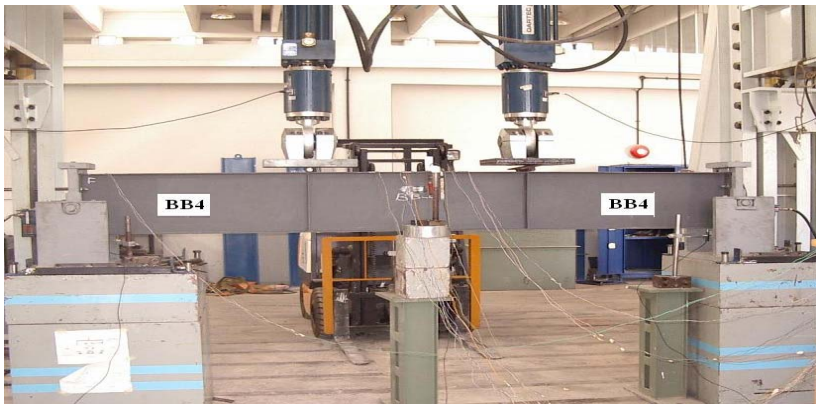

Figure (5): Buckling Test Apparatus.

120-EL were bonded to the specimens to measure localized strains. Four strain gages were located at mid span on the top and bottom fiber of the section to verify the bending moment within the span, and two strain gages were bonded to the web to detect the onset of local buckling of the web. An additional indication of the onset of the plate buckling was obtained by the concept of strain reversal using three pairs of electrical resistance strain gages mounted along the unsupported edges on opposite faces of the flange. A polished surface for each strain gage was prepared and cleaned prior to fixing the strain gage to the specimen. The locations of the measurements made for strain on the beam web and flanges are shown in Fig. (6).

Experimental Procedure

After each beam was prepared with its strain gages, it was placed onto the support and clamped in position by means of set screws threaded into the plate of the support. This had the effect of reducing warping of the end sections of the beams. The displacement transducers were set in place. The hydraulic jacks were carefully located and aligned as any eccentric loading would be undesirable. Both hydraulic jacks are connected to one servo-valve and hence apply equal loads. Since the load was applied using load control, particular care was

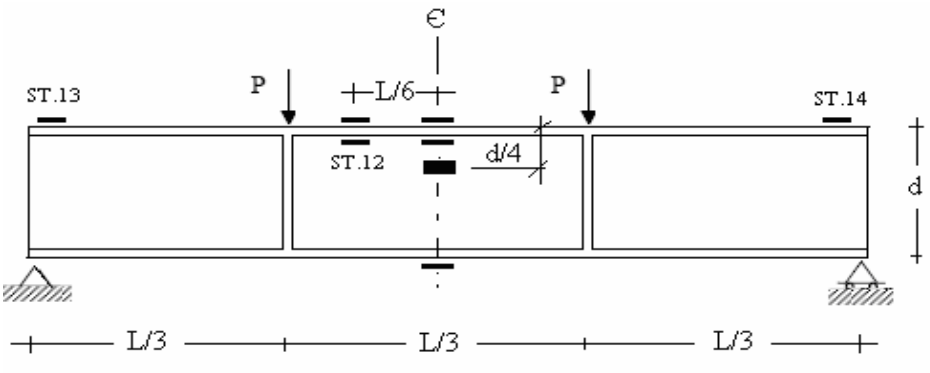

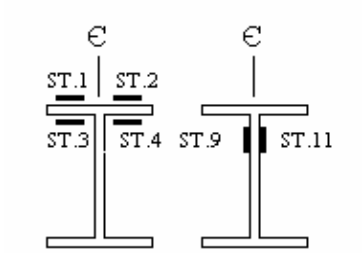

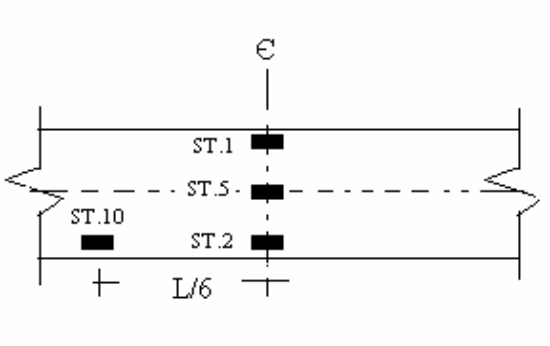

Top Flange

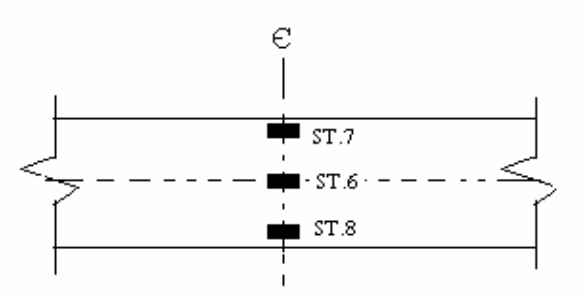

Bottom Flange

Figure (6): Strain Gage Identification Numbers and Locations.

required to accurately determine the ultimate loads without catastrophic failure. The test load was applied in increments, the size and rate of application of which depends on the proximity to failure estimated from the development of inelasticity and the growth of buckling deformations. The experiments proceeded with trail loading in the elastic range, up to about one third of the predicted failure load to ensure proper functioning of the instruments. Increments of 10 kN were applied in the early loading stages and were gradually reduced to 0.5 kN as the maximum load was neared. At every load step in the elastic range, a check of static equilibrium was obtained from the load cell reading, thereby assuring that the system was functioning properly. The magnitude of the applied constant bending moment within the span of the specimens was obtained by multiplying the jack load by the distance of the jack from the support (L/3). This value was compared with the bending moment calculated using the measured midspan strains (average of top and bottom flange strains). The agreement was good in all cases in the elastic range. The output from electrical resistance strain gages, LVDTs, cable transducers and load cells, amounting to as many as twenty one channels were recorded automatically at each step during the test on the data acquisition system at a rate of five readings per second . The failure mode was carefully observed. Buckling was deemed to occur when a load-deflection curve or lateral-deflection curve of one of the flange cross sections reached a horizontal asymptote. Even after each beam reached the ultimate strength point, tests were continued for a period of time to record the gradual unloading path.

TEST RESULTS AND DISCUSSION

Load-Strain Behavior and Strain Distribution

In Figs. (7) and (8) for specimens AB1 and AB1A in the first group are plotted the test load versus flange strains of the outer (1 and 2) and inner (3 and 4) strain gage pairs on the top flange and outer pairs of gages (7 and 8) on the bottom flange, respectively, of the station located at 1 m from end supports. The general behavior of these curves is the same. At relatively small loads, strains due to the strong axis bending dominate. The inner and outer top flange strains increase linearly with load and are about the same in compression and of opposite sign to bottom flange strains in tension. As soon as the beam begins to buckle laterally, the strains on the same flange but on opposite sides of the webs begin to diverge as lateral bending takes place. For beam AB1A, readings of the two strain gages (2 and 4) on the side of buckling direction decrease due to tensile strain from out-of-plane bending, while readings of the two strain gauges (1 and 3) on the opposite side increase in compression. When plate bending arising from local buckling takes place, a discrepancy between the strains on both surfaces appears, and finally, strain reversal at the convex side of the plate bending can be observed. The diverging strain readings in beam AB1A (1 and 3), (2 and 4) and (10 and 12) with one gage in tension and the other gage in compression indicate that local buckling occurred before ultimate loads were reached. Readings of the strain gages mounted in the bottom flange, gages 7 and 8, tend to develop tensile strains. Strain gage 8 and strain gage 2 on the top flange are on the same side of the web. As buckling was approached, both showed tensile straining, indicating that the lateral bending effect, in this case, was more pronounced that warping.

The load versus quarter-height web strains obtained from gages 9 and 11, 1 m from the end supports for specimen AB1A, is given in Fig. (8). The diverging strain readings with one gage in tension and the outer gage in compression indicate that out-of-plane bending of the web or web local buckling begins at a load of 80 kN. In all cases, the load versus strain relationship reaches a horizontal asymptote at the maximum load, indicating that buckling is imminent. The modes of failure for all the beams in the five groups are summarized in Table (3).

Behavior of Specimens and Failure Loads

In the AISC-LRFD (2003) specifications, the nominal bending strength of non-compact I-shaped beams is determined by the lowest value obtained according to the limit states of: Lateral-Torsional Buckling (LTB); Flange Local Buckling (FLB) and Web Local Buckling (WLB).

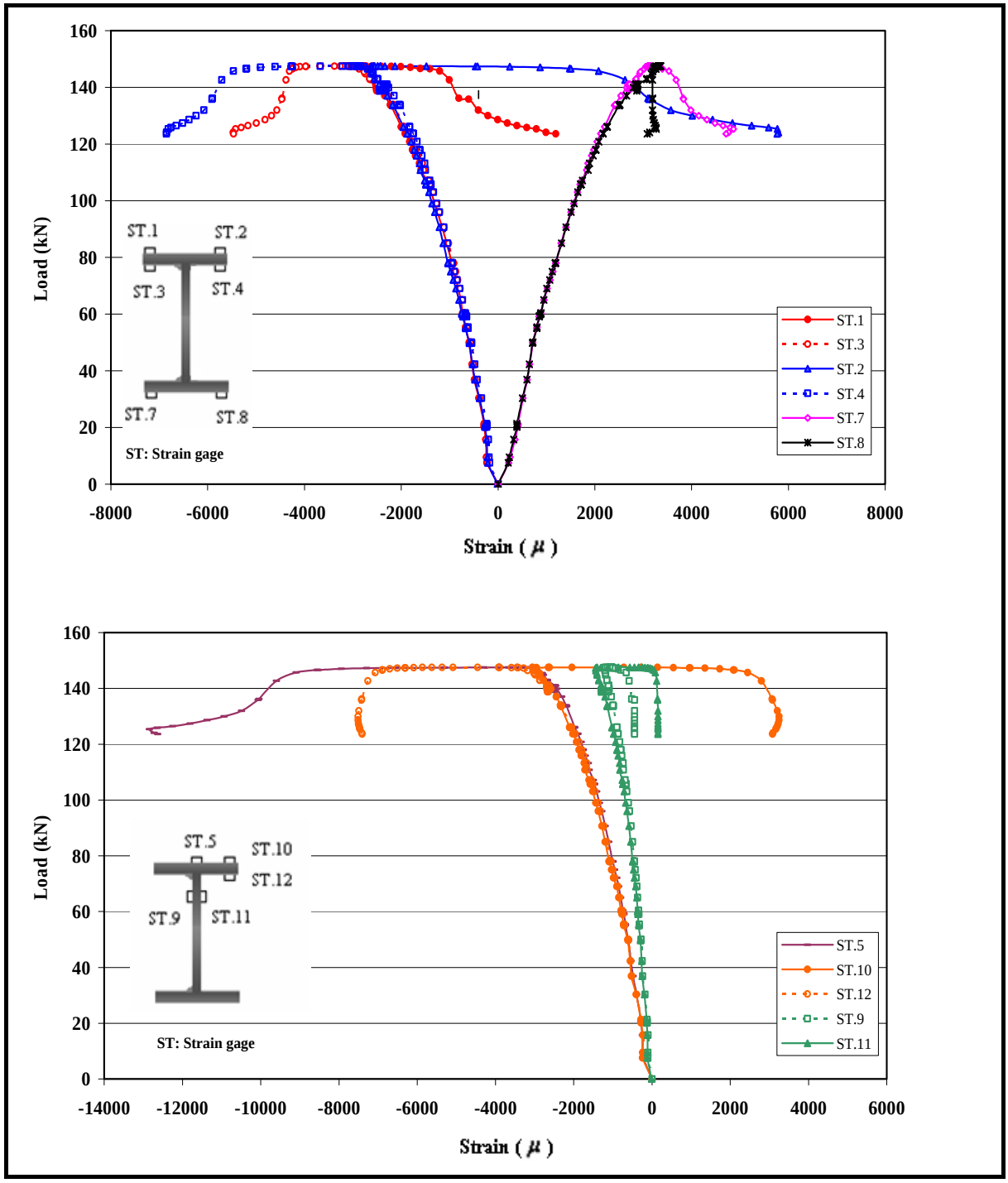

Figure (7): Load-Strain Curves for Beam AB1.

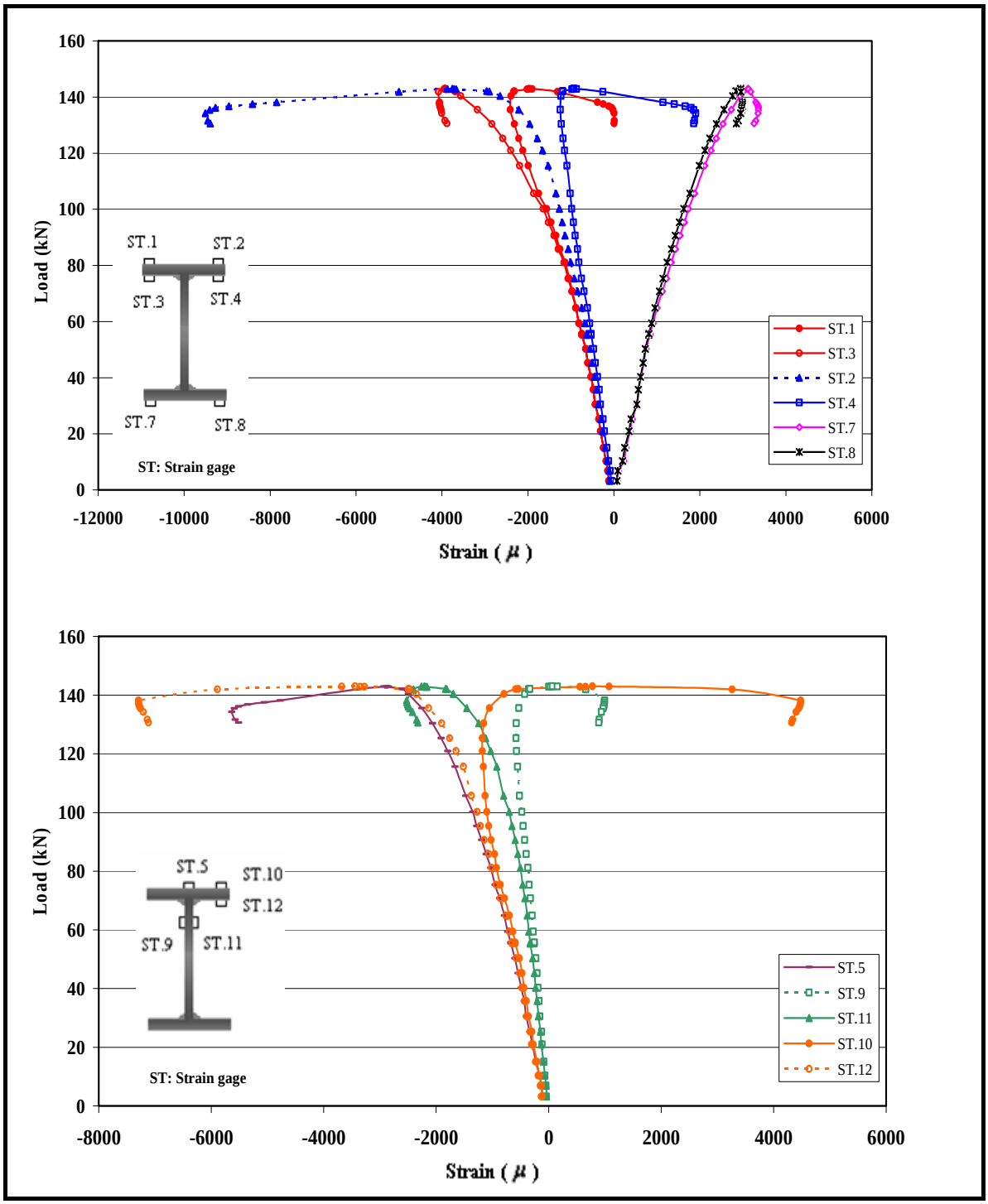

Figure (8): Load-Strain Curves for Beam AB1A.

Table (3): Failure Loads and Failure Modes.

Group	Specimens	Experimental			M_u / M_p	AISC LRFD Specification	
		P_u	M_u	Failure Mode		M_n	Failure
		(kN)	(kN.m)	modes		(kN.m)	modes
	AB1	147.55	98.37	FLB	0.81	95.45	FLB
1	AB2	141.46	94.24	FLB	0.77	95.51	FLB
	AB1A	142.97	95.31	Combined	0.77	96.1	FLB
	AB2A	140.70	93.80	Combined	0.75	99.11	FLB
	BB1	244.62	163.08	Combined	0.79	174.92	FLB
2	BB2	245.36	163.57	Combined	0.78	178.34	FLB
	BB1A	259.46	172.97	Combined	0.82	178.32	FLB
	BB2A	275.10	183.40	Combined	0.87	180.19	FLB
	AB3	95.12	95.12	FLB	0.80	85.20	LTB
3	AB3A	92.24	92.24	Combined	0.77	84.87	LTB
	AB4A	90.22	90.22	Combined	0.76	85.89	LTB
	BB3	163.72	163.72	FLB	0.77	143.46	LTB
4	BB4	168.50	168.50	FLB	0.80	141.56	LTB
	BB3A	175.70	175.70	Combined	0.83	142.82	LTB
	BB4A	197.70	197.70	Combined	0.93	142.34	LTB
	CB3	257.53	257.53	LTB	0.97	185.89	LTB
5	CB4	247.16	247.16	LTB	0.94	184.77	LTB
	CB3A	246.04	246.04	LTB	0.92	186.74	LTB
	CB4A	206.44	206.44	LTB	0.77	186.65	LTB

The limit state of lateral-torsional buckling is checked using the following equations:

When $L_b \le L_P$ $\quad M_n = M_P = F_y Z \le 1{,}5 M_y$ (1)

When $L_p \le L_b \le L_r$

$$M_n = C_b \left[M_P - (M_P - M_r)\left(\frac{L_b - L_P}{L_r - L_P} \right) \right] \le M_P \quad (2)$$

When $L_b \ge L_r$ $\quad M_n = M_{cr} \le M_p$ (3)

Assuming λ to be the controlling slenderness parameter (representing flange slenderness for flange local buckling or web slenderness for web local buckling limit states), the local buckling limit states are checked as follows:

when $\lambda_b \le \lambda_P$ $\quad M_n = M_P$ (4)

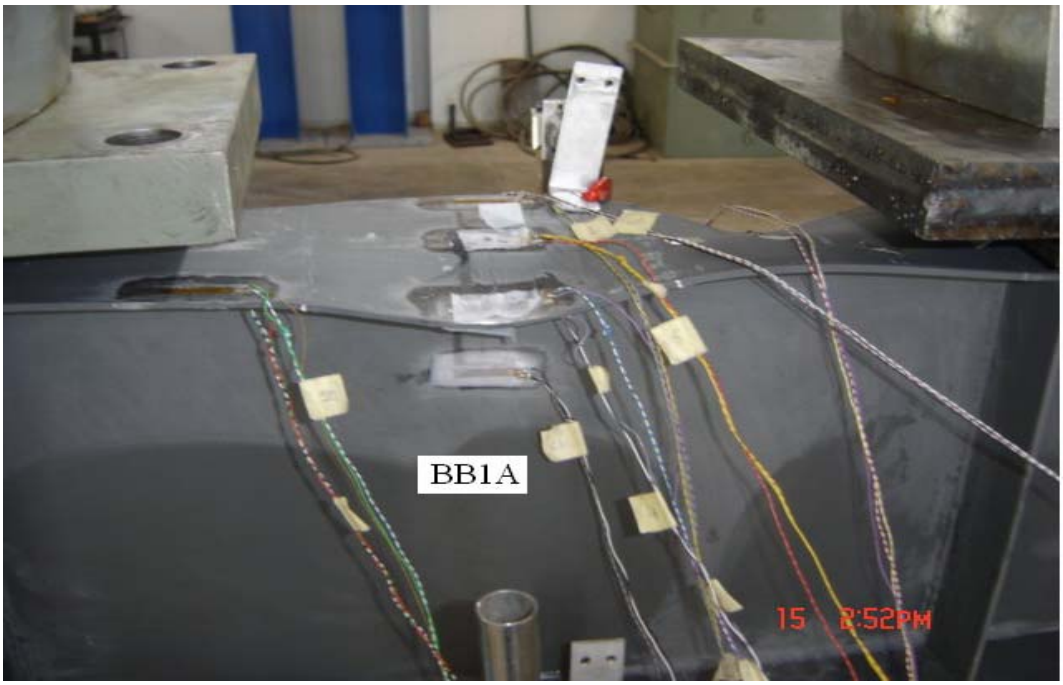

Figure (9): Combined Buckling Mode in Beam AB1A.

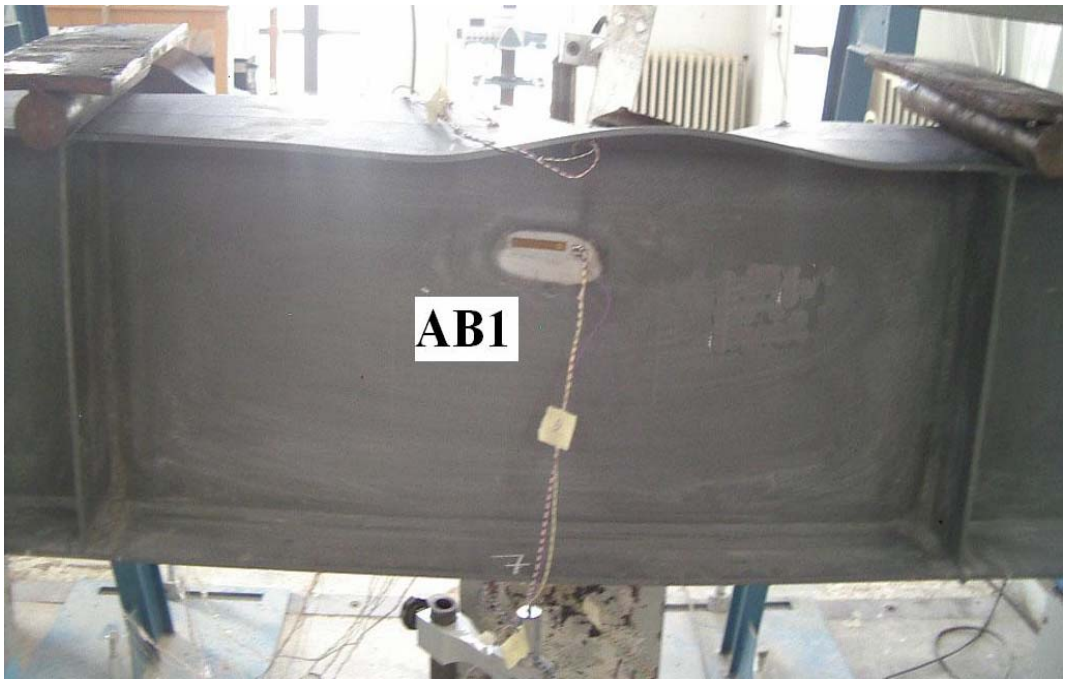

Figure (10): Local Buckling Mode in Beam AB1.

Figure (11): Lateral-Torsional Buckling Mode in Beam CB4A.

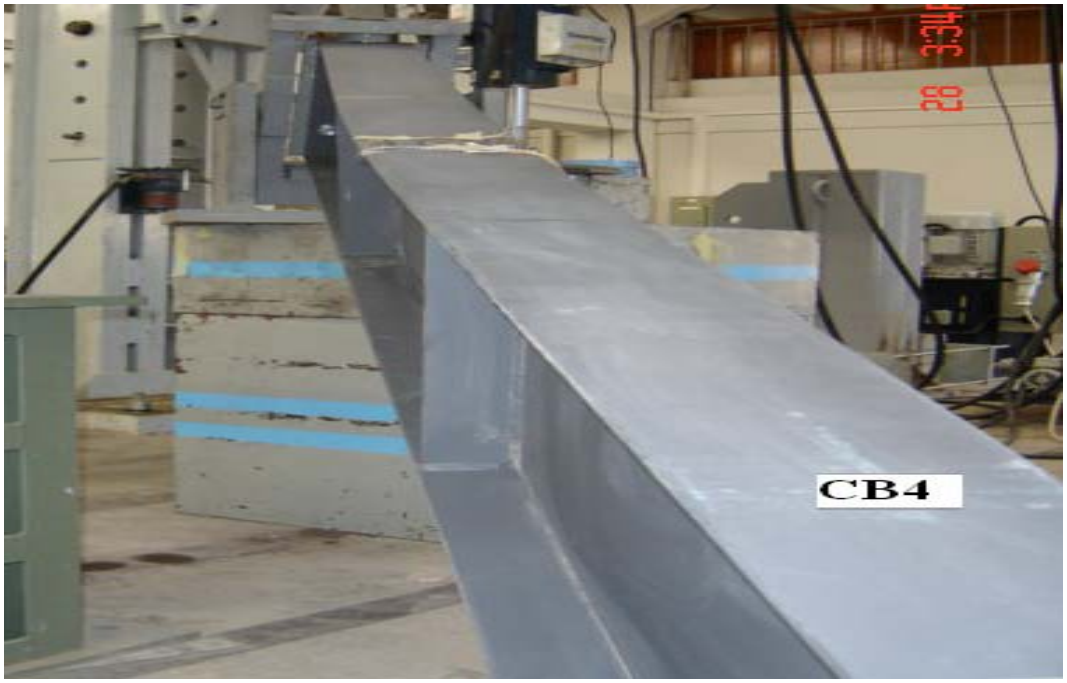

Figure (12): Lateral-Torsional Buckling Mode of Beam CB4.

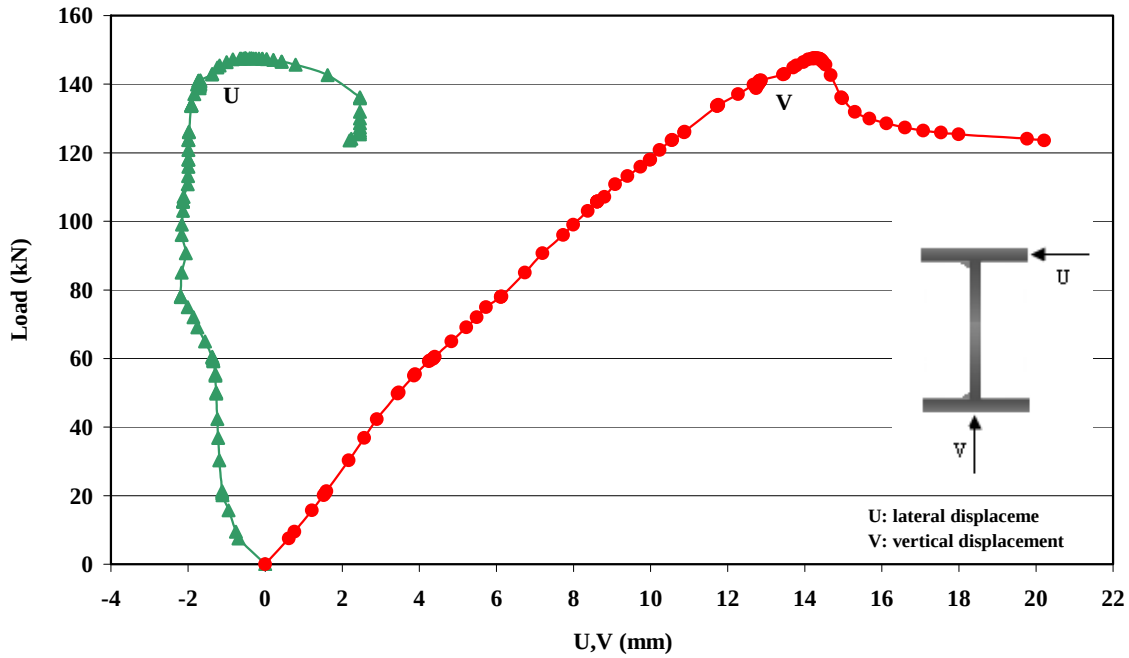

Figure (13): Load-Deflection Curves for Beam AB1.

when $\lambda_p \le \lambda_b \le \lambda_r$

$$M_n = C_b\left[M_P - (M_P - M_r)\left(\frac{\lambda_b - \lambda_P}{\lambda_r - \lambda_P}\right)\right] \le M_P \qquad (5)$$

where

λ_p Slenderness limits for compact.

λ_r Slenderness limits for non-compact.

The nominal bending strength M_n in the inelastic range and a summary of the experimental maximum loads, P_u, of all test beam are summarized in Table (3). Also shown are the modes of failure for the test beams and modes predicted by LRFD.

From the experimental failure loads of beams in the first group, shown in Table (3), it can be seen that the beams with fillet weld on one side of the web (FWO) showed a slight increase in strength over those of beams with fillet welds on both sides of the web (FWB). M_u / M_p of beam AB1 is 5% higher than its counterpart AB1A and that of beam AB2 is 3% higher than that of AB2A. The reason for this increase might be due to delayed yielding of the compression flange tips in beams with (FWO) because the compressive residual stresses near the flange tips are small. The local flange failure with a single wavelength was observed for beams with (FWO), as seen in Fig. (9) for beam AB1. For beams with (FWB), AB1A and AB2A, the local buckling and the lateral buckling are combined to produce a coupled mode of failure with a single wavelength for both local and lateral buckling as shown in Fig (10). A third mode of failure occurred only in beams with (FWB), this was web buckling. This can be explained due to the compression residual stresses in the web which precede yielding and thereby the reduction in effective cross-sectional stiffness.

The behavior of beams in the second group was influenced by the presence of residual stresses. Beams with (FWB) display higher strength than their counterpart beams with (FWO). When M_u / M_p values are compared, beam BB1A is 4% higher than its counterpart BB1 and BB2A is 12% higher than BB2, indicating that tensile residual stresses in the flange impart an improvement of approximately 8% for beams with

(FWB). A single wave in the longitudinal direction was observed for each beam in this group. Buckling of the web plates was observed at a load level of about 120 kN for beams with (FWB) and at a load level higher than 160 kN for beams with (FWO) in the same group.

The behavior of specimens in the third group was quite abrupt. Local buckling was dominant in the failure of AB3 while beams with (FWB) failed by combined local and lateral-torsional buckling. From Table (3), it can be seen that M_u / M_p of beam AB3 is 4% and 5% higher than its counterparts AB3A and AB4A, respectively.

Beams BB3A and BB4A in the fourth group failed by combined local flange and lateral–torsional buckling. Local buckling failure with one wave was observed for beams with (FWO). Table (3) clearly shows the improvement of lateral buckling capacity of beams with (FWB). The presence of tensile residual stresses in these beams seems to have a beneficial effect on their strength in comparison with their counterparts with (FWO). M_u / M_p of beam BB3A is 8% higher than that of beam BB3 and that of beam BB4A is 16% higher than that of beam BB4, indicating that tensile residual stresses in compression flange impart an improvement of 12% on average for beams with (FWB).

Lateral-torsional buckling was the primary mode of failure for the beams in the fifth group. Figs. (11) and (12) show the buckling mode of beam CB4A and its counterpart CB4, respectively. Buckling of web plates was not observed on any of the test beams in this group.

Load-Deflection Behavior

By monitoring the load deflection behavior during the test, deformation control could be invoked as the buckling load was approached. Buckling was considered to occur when the load-deflection curves reached a horizontal asymptote. The general behaviors of all specimens are approximately the same. From an examination of load-deflection curves of beam AB1 plotted in Fig. (13), it can be seen that the response is linear-elastic until the load reaches 40 kN where it jumps on to another linear response curve of only slightly lower relative stiffness. The behavior proceeds smoothly until buckling occurs and the load deflection curves reach a horizontal asymptote.

Support Conditions

The behavior of specimens of large slenderness was significantly influenced by the presence of end-plate connection which reduces warping. It is also apparent that the bolted end-plated connections provide a considerable improvement in buckling loads over simply supported end conditions which are free to warp. For built-up beams with high slenderness, the improvements in the buckling moment over the nominal moments predicted by LRFD (2003) as shown in Table (3) are 9%, 24% and 29% for the third, fourth and fifth groups, respectively. For the first and the second groups' specimens with lower slenderness, the beneficial effect of end-plate connections is not noticeable. This result conforms to that reported by Bradford and Trahair (1981). For short-length beams, where the flange of in-plane stiffness is high, buckling occurs in an antisymmetric mode in which the compressive flange deflects laterally as a near-rigid body while for long beams, this antisymmetric mode requires an excessive amount of strain energy to be stored in the web. Because of this, the beam prefers to buckle in symmetric mode in which little strain energy is stored in the web.

Evaluation of Test Results

Based on the recorded data and observation during testing which were described in the previous chapter, the ultimate bending moments, $M_u = P_u L/3$, obtained from all the tests are summarized in Table (4). The non-dimensional ultimate strength, M_u / M_y and M_u / M_p, and the modified slenderness ratio, $\bar{\lambda} = \sqrt{M_p / M_e}$ are also given. M_P is the full plastic moment calculated using the main yield stress and the measured cross sectional dimensions of each specimens. The theoretical critical moment for the elastic lateral buckling M_e was computed from Timoshenko and Gere (1961).

Table (4): Summary of Test Results.

Group #	Specimen	M_u kN.m	M_u / M_y	M_u / M_p	$\bar{\lambda} = \sqrt{M_p / M_e}$
1	AB1	98.37	0.90	0.81	0.73
	AB2	94.24	0.86	0.77	0.73
	AB1A	95.31	0.86	0.77	0.74
	AB2A	93.80	0.83	0.75	0.74
2	BB1	163.08	0.90	0.79	0.78
	BB2	163.57	0.89	0.78	0.78
	BB1A	172.97	0.94	0.82	0.78
	BB2A	183.40	0.99	0.87	0.78
3	AB3	95.12	0.88	0.80	1.09
	AB3A	92.24	0.86	0.77	1.10
	AB4A	91.22	0.84	0.76	1.09
4	BB3	163.72	0.88	0.77	1.15
	BB4	168.50	0.92	0.80	1.15
	BB3A	175.70	0.94	0.83	1.15
	BB4A	197.70	1.06	0.93	1.16
5	CB3	257.53	1.09	0.97	1.11
	CB4	247.16	1.05	0.94	1.11
	CB3A	246.04	1.03	0.92	1.11
	CB4A	206.44	0.87	0.77	1.12

Comparison with Available Test Data of Welded Beams

It may be observed from Fig. (14), in which the available test data for welded beams are plotted (Fukumoto and Itoh, 1981; Kubu and Fukumoto, 1988) and when all such test points are enclosed by a convex chain-line boundary, that fourteen of the test points from the present test groups lie inside this chain, highlighting the strong influence of the present test variables. Also, this demonstrates that the plotted results of the test groups are very close to the previous results of specimens which are comparable. The other five specimens with large $\bar{\lambda}$ are significantly stronger than welded beams from previous tests of equal slenderness. The strength capacity is of the order 11-17%.

Comparison with Available Test Data of Rolled Beams

Fukumoto and Kubo (1977) carried out an extensive survey of literature on the lateral buckling tests that had been conducted at various institutions. In Fig. (15), the present test results for the five groups are compared with the past 128 test points for rolled sections. The clear trend for the test results in the first and second groups indicates

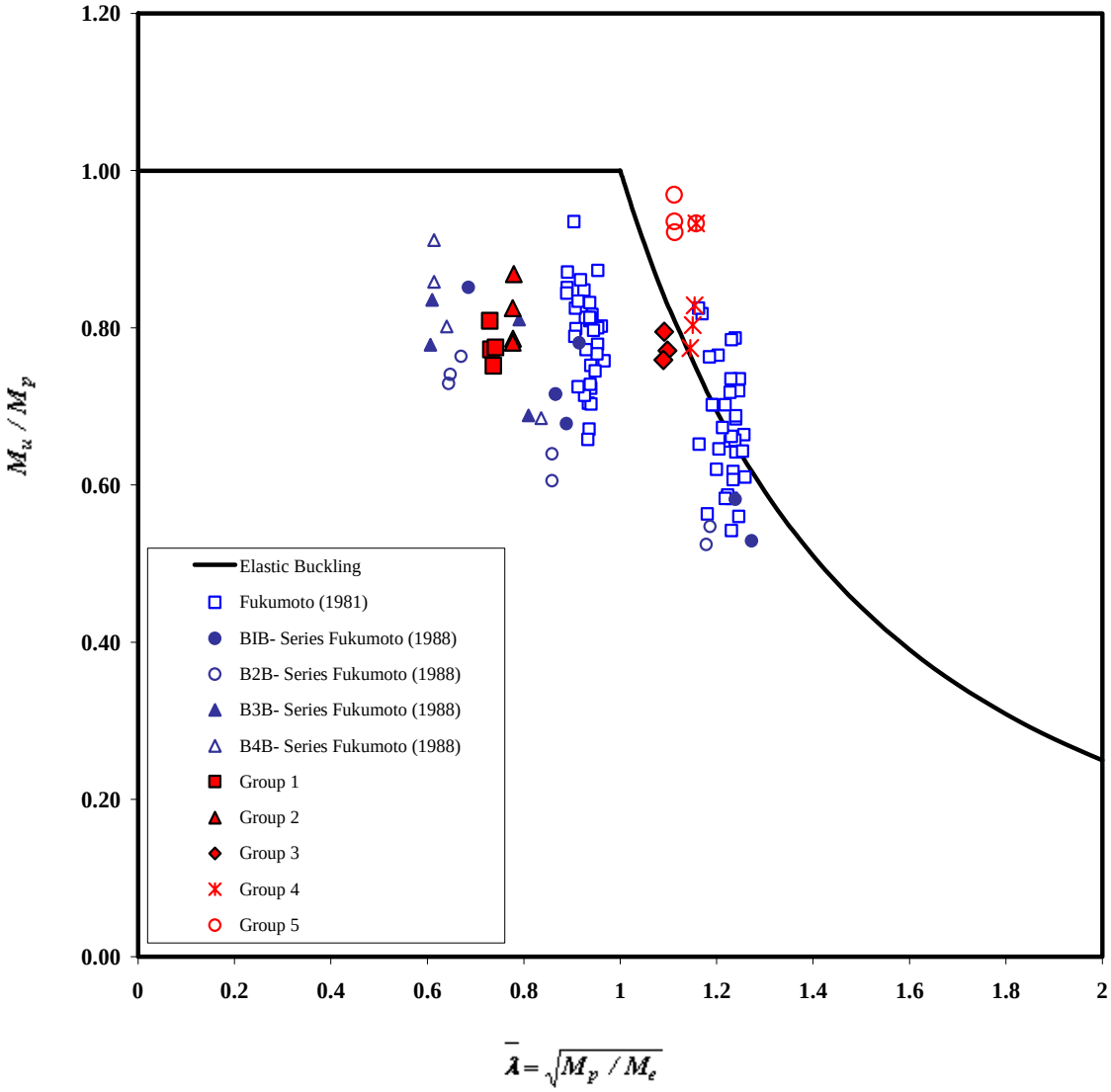

Figure (14): Comparison of Test Results with Available Test Data for Welded Beams.

that built-up beams are weaker than rolled beams of equal slenderness for levels of slenderness in the range of $\bar{\lambda} \le 0.8$. It may be due to the variation in the compressive residual stresses and initial lateral crookedness. In the range of large $\bar{\lambda}$, the test results show higher ultimate strength than rolled beams. It may be explained by the difference in support conditions.

Comparison with Current Standards

The M_u / M_p versus the modified slenderness curves are plotted in Fig. (16) together with the test values. It can be seen from Fig. (16) that the predicted lateral strengths from the LRFD specification (2005) are higher than the test values for small values of $\bar{\lambda}$ and lower than the test values for large values of $\bar{\lambda}$. The predictions in CSA-S16-01 (2001), which are based on the upper bound of

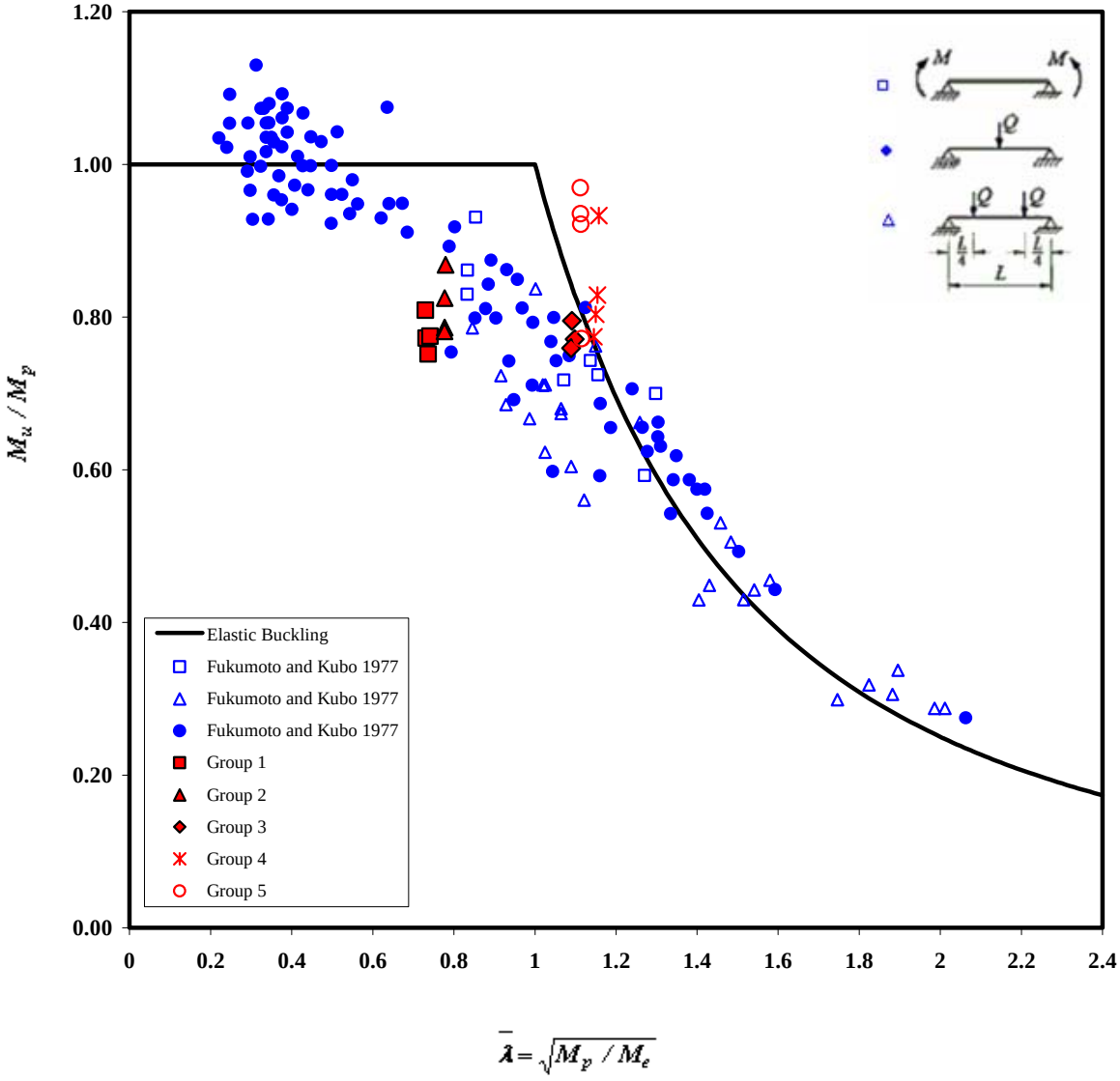

Figure (15): Comparison of Test Results with Available Test Data for Hot Rolled Beams.

the test values of I-section beams, are lower than the test values. The predictions of Eurocode 3 (2003), Part 1.1 are lower than the test values for large values of $\bar{\lambda}$. The Australian Standard AS4100 (1998) gave the most conservative predictions and provided good lower bound estimates to the failure loads of the built-up beams, because it is based on the lower bounds of the test values of I-section beams. The design rules in different standards for lateral-torsional buckling of beams are based on test results of beams restrained at their supports against torsion but not against warping. In the current study, especially for the fourth and the fifth groups, an improvement in buckling strength was observed due to the bolted end connections which reduce warping.

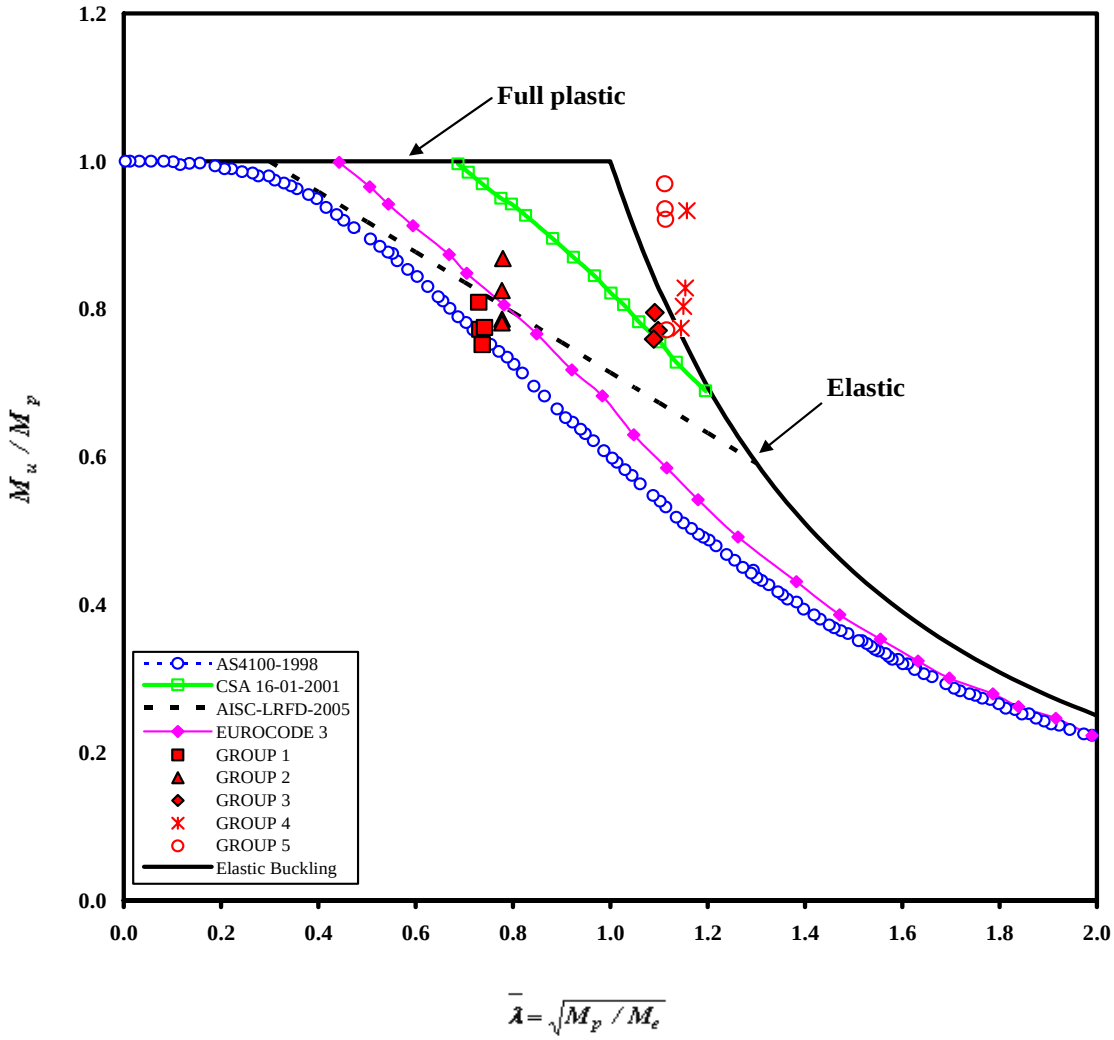

Figure (16): Comparison of Test Results with Current Standards.

CONCLUSIONS

Regarding the experimental results and observations, the following conclusions can be drawn.

1. For relatively large $\bar{\lambda}$, about 1.1, when flange thickness to web thickness ratio (t_f / t_w) equals 1.2 (for the second and the fourth groups), the combined failure mode of local flange buckling and lateral-torsional buckling was obtained for beams with fillet weld on both sides of the web, while the beam with fillet weld on one side of the web failed only by local flange-buckling. In the range of intermediate $\bar{\lambda}$, about 0.78, local flange-buckling and local web-buckling were the primary modes of failure.
2. For large and intermediate $\bar{\lambda}$, when the ratio of thicknesses of the flange to the web, t_f / t_w = 1.25 (for the first and the third groups), the combined failure mode of local flange and lateral-torsional buckling was observed for beams with fillet weld on both sides of the web, while beams with fillet weld on one side of the web failed only due to local buckling of the flange.
3. For relatively large $\bar{\lambda}$, about 1.1, when t_f / t_w equals 1.33 (for the fifth group), lateral torsional-

buckling was the primary mode of failure.

4. The ultimate strengths of built-up sections with fillet welds on both sides of the web are not always greater than their counterpart beams with fillet weld on one side of the web.
5. The bolted end-plate connection at the beam ends may induce end-restraining moments that oppose the warping deformation and modify the lateral buckling resistance of the beam especially for high slenderness ratios, $\overline{\lambda} \geq 1.1$.
6. The design curves for various codes vary markedly. The design loads predicted by the AS4100 (1998) provided good lower bound estimates to failure loads of the tested beams.

NOTATION

E	Elastic modulus
F_u	Maximum stress
F_Y	Yield stress
M_{cr}	Critical elastic lateral-torsional buckling moment
M_e	Elastic buckling moment
M_n	Nominal section capacity
M_n	Nominal section capacity
M_P	Full plastic moment
MPa	Mega Pascal
M_u	Ultimate moment
$\overline{\lambda}$	Modified slenderness ratio
λ_p	Slenderness limits for compact
λ_r	Slenderness limits for non-compact
ν	Poisson's ratio

REFERENCES

American Institute of Steel Construction. 2003. Load and Resistance Factor Design Specification for Structural Steel Buildings.

American Welding Society. 2000. Structural Welding Code-Steel, American National Standards Institute/ American Welding Society (ANSI/AWS), D1.1-2000.

ASTM Standard E8. 2003. Standard Test Methods and Definitions for Mechanical Testing of Steel Products.

ASTM Standard E837. 2001. Standard Test Method for Determining Residual Stresses by the Hole-Drilling Strain Gage Method.

Bradford, M. A. and Trahair, N. S. 1981. Distorsional Buckling of I-beams. *Journal of Structural Division*, ASCE, 107 (2): 335-370.

Canadian Standard Association. 2001. Steel Structure for Building (Limit State Design). CAN/CSA-16-01, Rexdale, Ontario, Canada.

Eurocode 3. 2005. Design of Steel Structures: Part 1.1- General Rules and Rules for Buildings. DD ENV, 1993-1.1.

Fukumoto, Y. and Kubo, M. 1977. A Survey of Tests on Lateral Buckling Strength of Beams. European Convention for Constructional Steel Work, Preliminary Report, Second International Colloquium on Stability of Steel Structures, Liege, Belgium, 233-240.

Fukumoto, Y., Itoh, Y. and Kobo, M. 1980. Strength Variation of Laterally Unsupported Beams. *Journal of Structural Division*, ASCE, 106 (ST1): 165-181.

Fukumoto, Y. and Itoh, Y. 1981. Statistical Study of Experiments on Welded Beams. *Journal of Structural Division*, ASCE, 107 (ST1): 89-103.

Fukumoto, Y., Itoh, Y. and Hattori, R. 1982. Lateral Buckling Tests on Welded Continuous Beams. *Journal of Structural Division*, ASCE, 108 (ST10): 2245-2262.

Galambos, T.V. 1998. Guide to Stability Criteria for Metal Structure, 5th Ed., New York: John Wiley and Sons.

Kubo, M., Itoh, Y. and Fukumoto, Y. 1988. Lateral-Torsional Buckling of Thin-Walled I-Beams. *Journal of Structural Engineering*, ASCE, 114 (4): 841-855.

Standard Association of Australia (SAA). 1998. Steel Structures. Australian Standard AS4100, Sydney, Australia.

Timoshenko, S.P. and Gere, J.M. 1961. Theory of Elastic Stability. McGraw-Hill, New York.

Trahair N.S. 1993. Frexural-Torsional Buckling of Structures, Chapman and Hall, London.